Monatshefte für Chemie 130, 1207–1216 (1999)

Monatshefte für Chemie
Chemical Monthly

Perchlorate Pitting Corrosion of a Passivated Silver Electrode

Sayed S. Abd El Rehim*, **Hamdy H. Hassan, Magdy A. M. Ibrahim,** and **Mohammed A. Amin**

Chemistry Department, Faculty of Science, Ain Shams University, Cairo, Egypt

Summary. The passivation and pitting breakdown of a silver electrode in sodium hydroxide solutions containing sodium perchlorate was studied using potentiodynamic and potentiostatic techniques. In perchlorate-free alkali solution, the voltammogram exhibits three anodic peaks prior to oxygen evolution. The first two peaks correspond to the oxidation of Ag and formation of a passive film of Ag_2O on the electrode surface, the third to the conversion of Ag_2O to AgO. In the presence of ClO_4^-, the voltammogram depends considerably on perchlorate concentration. ClO_4^- increases the height of the three anodic peaks, and at potentials above a limiting value breakdown of the anodic passivity and initiation of pitting corrosion occurs. The pitting potential decreases linearly with ClO_4^- concentration but increases with scan rate. The potentiostatic current/time transients show that pitting corrosion can be described in terms of an instantaneous three dimensional growth under diffusion control.

Keywords. Pitting corrosion; Silver anode; Perchlorate anion.

Perchloratinduzierte Lochfraßkorrosion an einer passivierten Silberelektrode

Zusammenfassung. Passivierung und Lochfraßkorrosion einer Silberelektrode in Natriumperchlorat enthaltenden Natriumhydroxidlösungen wurden mit potentiodynamischen und potentiostatischen Methoden untersucht. In perchloratfreier alkalischer Lösung zeigt das Voltammogramm vor Beginn der Sauerstoffentwicklung drei anodische Peaks. Die ersten beiden entsprechen der Oxidation von Ag und der Bildung einer passivierenden Ag_2O-Schicht auf der Elektrodenoberfläche, der dritte einer Umwandlung von Ag_2O in AgO. In Gegenwart von ClO_4^- wurde eine ausgeprägte Abhängigkeit der Voltammogramme von der Perchloratkonzentration festgestellt. Durch die Anwesenheit von ClO_4^- wird die Intensität der drei anodischen Peaks erhöht, und ab einem gewissen Potential bricht die Passivierung unter Eintreten von Lochfraßkorrosion zusammen. Das Lochfraßpotential nimmt linear mit der Konzentration von ClO_4^- ab und steigt mit der Scangeschwindigkeit. Die potentiostatischen Strom/Zeit-Diagramme zeigen, daß die Lochfraßkorrosion als diffusionskontrolliertes dreidimensionales Wachstum charakterisiert werden kann.

Introduction

The anodic behaviour of silver in alkaline solutions has been extensively studied [1–7], in particular due to the use of silver electrodes in various types of alkaline

* Corresponding author

and sea water batteries and the nucleation and growth of AgO on Ag/Ag_2O substrates serving as cathodes in Ag-Zn alkaline batteries [1–3]. According to our knowledge, no work has been published on breakdown of silver passivity and initiation of pitting corrosion in alkaline solution. Therefore, the influence of perchlorate ions as aggressive species on the passivation and pitting corrosion of silver in sodium hydroxide solution over certain ranges of concentration, scan rate, and applied potential was studied using potentiodynamic and potentiostatic techniques.

Results and Discussion

Potentiodynamic polarization measurements

Figure 1 shows the anodic potentiodynamic voltammogram for Ag in 0.5 *M* NaOH at a scan rate of $100\,mV \cdot s^{-1}$. It exhibits a complex shape characterized by the contribution of the three anodic peaks (A_1, A_2, A_3) prior to oxygen evolution reaction. The peaks in the voltammogram are virtually the same as those found in the literature [8–11]. The first peak (A_1), located at about 225 mV (SCE), can be assigned to the anodic oxidation of Ag to $[Ag(OH)_2]^-$ by adsorption of OH^- and desorption of the products.

$$Ag + 2OH^- = [Ag(OH)_2]^- + e^-$$

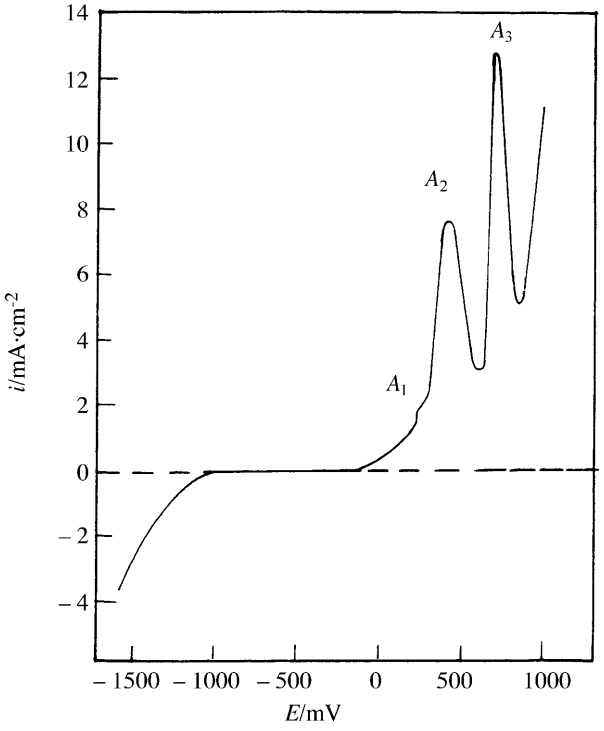

Fig. 1. Typical voltammogram of an Ag electrode in 0.5 *M* NaOH between $E_{s,c} = -1600\,mV$ and $E_{s,a} = 1000\,mV$ at 25°C and at a scan rate of $10\,mV \cdot s^{-1}$

When the concentration of this complex exceeds the solubility product of Ag_2O, precipitation of a monolayer of this oxide occurs on the electrode surface. The second peak (A_2), located at about 400 mV, is related to the direct formation and thickening of an Ag_2O multilayer from Ag.

$$2Ag + 2OH^- = Ag_2O + H_2O + 2e^-$$

When the thickness of the Ag_2O layer reaches a certain value, the current density drops to a small value, indicating the onset of primary passivity; this region extends to about 650 mV. Above this potential, the current density starts to increase and forms peak A_3 which is due to conversion of Ag_2O to AgO.

$$Ag_2O + 2OH^- = 2AgO + H_2O + 2e^-$$

At the end of the conversion process, the current density decreases, forming a secondary passivation region prior to oxygen evolution.

The influence of the addition of increasing amounts of $NaClO_4$ (0.1 to 0.6 *M*) on the anodic voltammogram of Ag in 0.50 *M* NaOH is shown in Fig. 2. The voltammograms depend considerably on ClO_4^- concentration. In general, the addition of ClO_4^- increases the height of the three anodic peaks as well as the current densities in the passive regions. The relation between the peak current density of peak $A_2(i_{pA_2})$ and the logarithm of the ClO_4^- concentration is given in Fig. 3. The accelerating influence of ClO_4^- on peak A_2 can be ascribed to the formation of soluble $AgClO_4$. Therefore, in terms of an adsorption model, it can be conclude that both OH^- and ClO_4^- are likely to become adsorbed on the metal surface [12–14], forming a potentially active dissolution site. It seems that the subsequent anodic dissolution process involves both the formation of an Ag_2O film and of soluble $AgClO_4$. The extent of the two processes depends upon the relative abundance of the two ions in the solution.

However, the addition of low concentrations of ClO_4^- ($< 0.40\,M$) in 0.5 *M* NaOH breaks down the secondary AgO passive layer and initiates pitting corrosion at certain critical pitting potential E_{pit} more negative than oxygen evolution potential. It is probable that at E_{pit} the adsorbed ClO_4^- ions on the oxide/electrolyte interface penetrate the oxide film at localized point defects and flaws and attack the base metal, thus leading to a sudden rise in current density. The pitting potential shifts towards a more negative (active) direction with increasing ClO_4^- concentration. At ClO_4^- concentrations above 0.30 *M*, pitting corrosion occurs within the primary passivation region. However, with still higher ClO_4^- concentrations ($\geq 0.60\,M$) it seems that E_{pit} is reduced below the passivation potential, making the formation of anodic peaks impossible. Dissolution may occur uniformly (general corrosion) across the entire surface. A plot of E_{pit} *vs.* the logarithm of ClO_4^- concentration is given in Fig. 4.

Figure 5 illustrates the influence of the scan rate on the anodic behaviour of Ag in 0.5 *M* NaOH containing 0.4 *M* $NaClO_4$. Under the prevailing conditions, the increase in the scan rate (v) results in a marked increase of the height of the anodic peaks A_1 and A_2 and the current densities in the primary passive region. When v is high, an initiation of passivity breakdown can be noticed only at more positive potentials, corresponding to a sufficiently short pit incubation time [15]. The

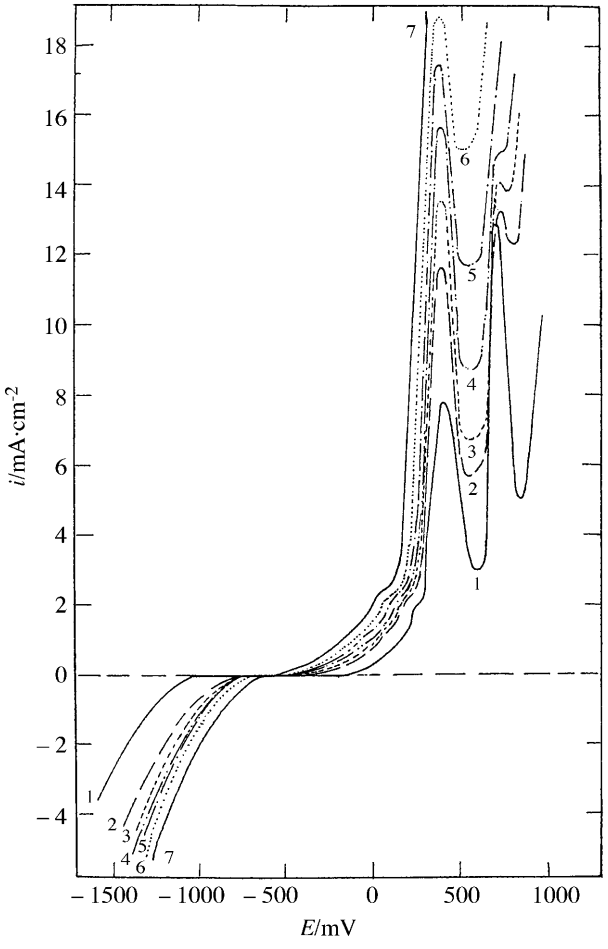

Fig. 2. Effect of addition of $NaClO_4$ on the voltammogram of an Ag electrode in 0.5 *M* NaOH between $E_{s,c} = -1600$ mV and $E_{s,a} = 1000$ mV at 25°C and at a scan rate of 10 mV · s^{-1}; (1) 0.0 *M* $NaClO_4$, (2) 0.1 *M* $NaClO_4$, (3) 0.2 *M* $NaClO_4$, (4) 0.3 *M* $NaClO_4$, (5) 0.4 *M* $NaClO_4$, (6) 0.5 *M* $NaClO_4$, (7) 0.6 *M* $NaClO_4$

incubation time for initiation of passivity breakdown, *i.e.* for a first pit nucleation, is caused by the time required for ClO_4^- pentration into the passive layer.

Current/time transient measurements

In order to get more information about the breakdown of the primary passivation (Ag_2O layer) by ClO_4^- ions, potentiostatic current/time transients at constant step potentials $E_{s,a}$ (within the primary passivation region) were recorded. Figure 6 shows the effect of the anodic step potential $E_{s,a}$ on the transients at a given concentration of ClO_4^- (0.4 *M*) in 0.5 *M* NaOH, whereas Fig. 7 demonstrates the effect of ClO_4^- concentration on the transients at a given $E_{s,a}$ (600 mV). The data of Fig. 6 infer that for $E_{s,a} < E_{pit}$ the current density decreases monotonically to a steady state value. If the contribution of the double layer charging process is

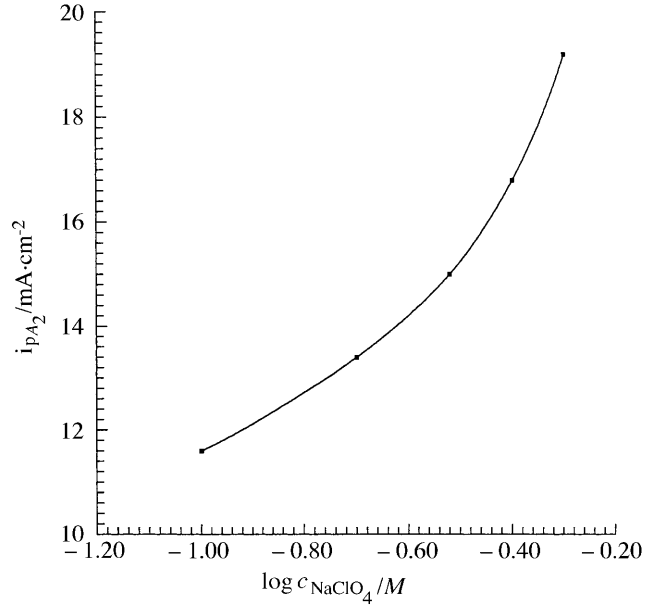

Fig. 3. Dependence of $i_P A_2$ on $\log c_{ClO_4^-}$ for an Ag electrode in 0.5 M NaOH

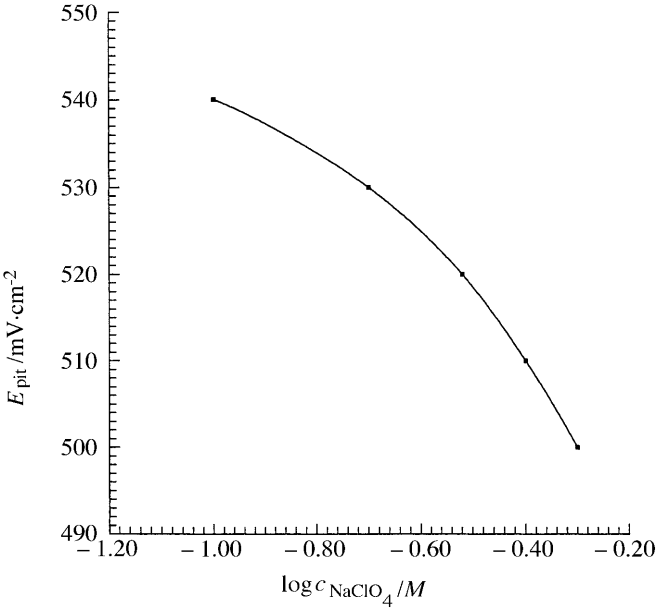

Fig. 4. Dependence of E_{pit} on $\log c_{ClO_4^-}$ for an Ag electrode in 0.5 M NaOH

neglected, the overall transient current density (i) can be assigned to two main processes: the passive layer growth (i_{gr}) and silver electrodissolution through the passive layer (i_{dis}):

$$i = i_{gr} + i_{dis}$$

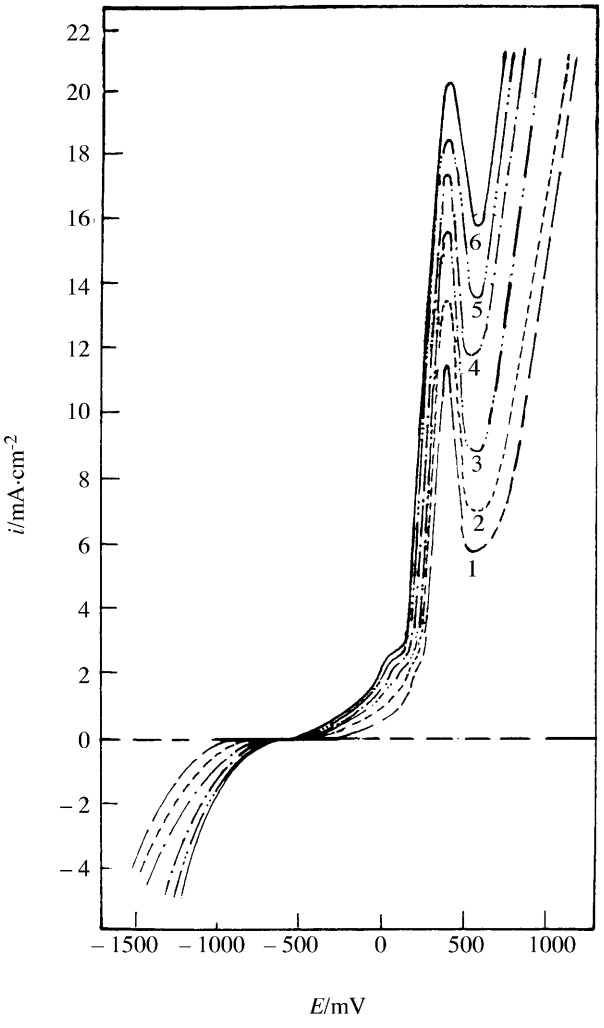

Fig. 5. Voltammograms of an Ag electrode in 0.5 *M* NaOH+0.4 *M* $NaClO_4$ between $E_{s,c} = -1600$ mV and $E_{s,a} = 1000$ mV at 25°C and at different scan rates; (1) 1 mV · s^{-1}, (2) 5 mV · s^{-1}, (3) 10 mV · s^{-1}, (4) 25 mV · s^{-1}, (5) 50 mV · s^{-1}, (6) 100 mV · s^{-1}

The growth of the passive layer can be regarded as the formation of a new solid phase (Ag_2O) on the metal surface. The silver electrodissolution through the passive layer can be explained in terms of Ag^+ diffusion from the metal/film interface to the film/solution interface [16]. These two processes can occur independently on the entire electrode surface.

For $E_{s,a} > E_{pit}$ the transition current density initially decreases to a minimum value at time t_i (incubation time), *i.e.* when the ClO_4^- ions penetrate the passive layer and reach the metal surface, pits start to grow, and the current rises steeply. In this case the overall transient current density is given by three contributions:

$$i = i_{gr} + i_{dis} + i_{pit}$$

i_{pit} is related to the pit growth current density, *i.e.* the rate of pitting corrosion, and follows a relationship with the square root of time as shown in Fig. 8.

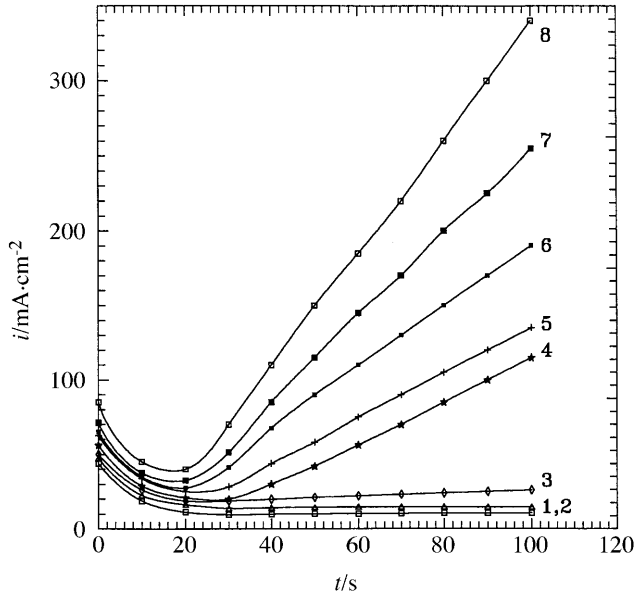

Fig. 6. Current transients at different step potentials $E_{s,a}$ recorded for a polycrystalline Ag electrode in 0.5 *M* NaOH containing 0.4 *M* $NaClO_4$ at 25°C and at a scan rate of $10\,mV \cdot s^{-1}$ starting at (1) 400 mV, (2) 450 mV, (3) 500 mV, (4) 550 mV, (5) 600 mV, (6) 650 mV, (7) 700 mV, (8) 750 mV

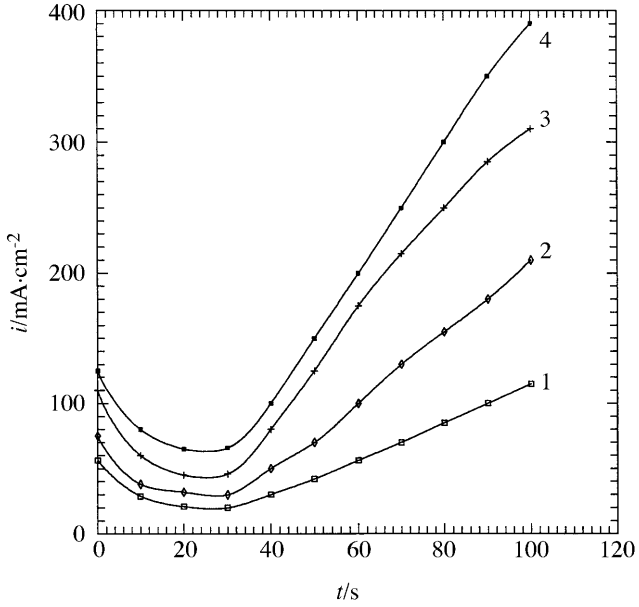

Fig. 7. Current transients at constant step potential $E_{s,a} = 550\,mV$ recorded for a polycrystalline Ag electrode in 0.5 *M* NaOH containing various amounts of $NaClO_4$ at 25°C and at a scan rate of $10\,mV \cdot s^{-1}$ starting at (1) 0.40 *M* $NaClO_4$, (2) 0.45 *M* $NaClO_4$, (3) 0.50 *M* $NaClO_4$, (4) 0.55 *M* $NaClO_4$

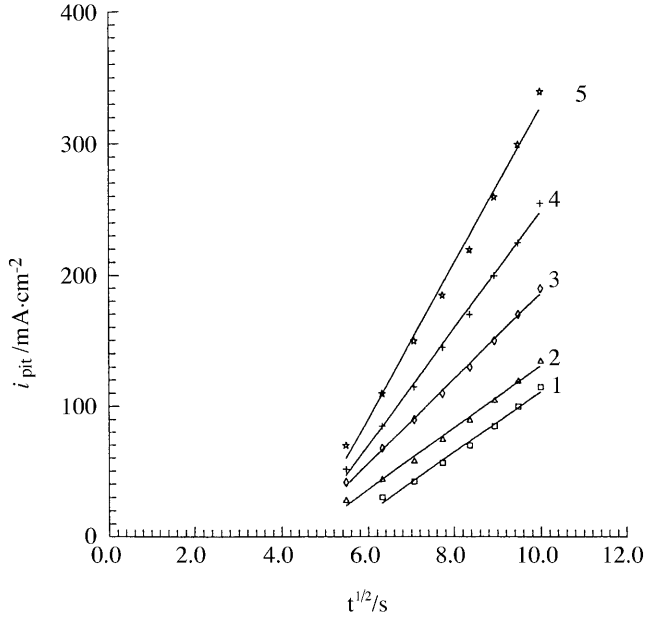

Fig. 8. Dependence of i_{pit} on $t^{1/2}$ for an Ag electrode in 0.50 *M* NaOH containing 0.40 *M* $NaClO_4$ at different step potentials $E_{s,a}$; (1) 550 mV, (2) 600 mV, (3) 650 mV, (4) 700 mV, (5) 750 mV

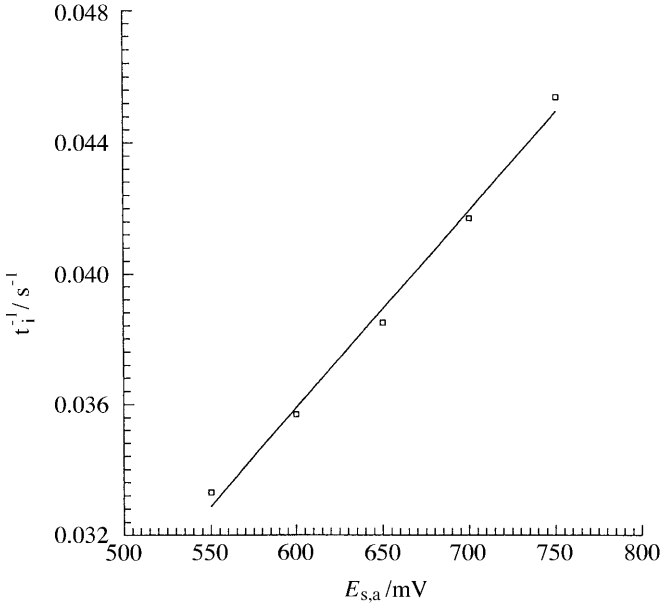

Fig. 9. Dependence of $1/t_i$ on $E_{s,a}$ for an Ag electrode in 0.50 *M* NaOH containing 0.40 *M* $NaClO_4$

These results agree well with *Hills* model [16] which can be described by the equation

$$i_{\text{pit}} = 2^{3/2} \cdot P \cdot t^{1/2}$$

where $P = zF\pi N_o D^{3/2} C^{3/2} M^{1/2} \rho^{1/2}$, N_o is the number of sites available for pitting corrosion, D, C, M, and ρ are the diffusion coefficient, the concentration, the molecular weight, and the density of the dissolved materials, and the other terms have their usual meaning. The current relationship with $t^{1/2}$ suggests that the pit growth is an instantaneous three-dimensional nucleation followed by growth controlled by diffusion. The dependence of the pitting growth current on the potential value indicates that there is a distribution of nucleation sites of different energies which nucleate at distinct potential [15]; in other words, the more positive the applied potential, the more activated sites will be present.

From the data of Fig. 8 it can be concluded that an incubation time is necessary before the pit nucleation and growth process to occur. The incubation time decreases with increasing potential step $E_{s,a}$. This observation can be confirmed by plotting the rate of ClO_4^- penetration defined as $(1/t_i)$ *vs.* $E_{s,a}$ [16]. The result is given in Fig. 9 where a straight line relationship is observed, indicating that the rate of penetration increases steadily with E_s. In addition, the data of Fig. 9 show that the rate of penetration increases (and, consequently, the incubation time decreases) with increasing ClO_4^- concentration at a given $E_{s,a}$.

Experimental

The working electrode used in the present study was made of spec pure polycrystalline silver (99.99%, Koch Light Laboratories, Colnbrook Bucks, England) axially embedded in an araldite holder to offer an active flat disc shaped surface (area: 0.1256 cm^2). Prior to each experiment, the working electrode was polished successively with fine grade emery papers. Then the polished metal surface was rinsed with acetone and distilled water and finally dipped in the electrolytic cell. a platinum wire was used as the counter electrode. A saturated calomel electrode (SCE) was used as a reference electrode to which all potentials are referred. All solutions were freshly prepared from analytical grade chemical reagents using doubly distilled water. Each run was carried out in aerated stagnant solution at room temperature (25±2°C).

Potentiodynamic polarization experiments were performed using a potentioscan type apparatus (Potentiostat/Galvanostat Model 273 EG&G) by changing the electrode potential automatically from the starting potential towards the positive direction at the required scan rate till the end of the experiment. The *E*/*i* curves were recorded using an X-Y recorder (Series 2000, Omnigraphic).

The anodic current transients at constant anodic step potentials $E_{s,a}$ were recorded in a two step procedure. The silver electrode was first held at the starting potential for 60 s to attain a reproducible electroreduced silver surface. Then the electrode was potentiodynamically polarized in the positive direction with a scan rate of 100 $mV \cdot s^{-1}$ to a step potential $E_{s,a}$ at which the current transient was recorded.

References

[1] Hoar TP, Dyer CK (1972) Electrochim Acta **17**: 1563
[2] Sato N, Shimizu Y (1973) Electrochim Acta **18**: 567
[3] Muller RH, Smith CG (1980) Surf Sci **96**: 375
[4] Bunstein GT, Newman RC (1980) Electrochim Acta **25**: 1009

[5] David MD, Ian MR, Pritam S, Zhang H-G (1989) Electrochim Acta **34**: 409
[6] Alonso C, Salvarezza RC, Vara JM, Arvia AJ (1990) Electrochim Acta **35**: 489
[7] Dirkse TP (1990) Electrochim Acta **35**: 1445
[8] Salvarezza RC, Becerra JG, Ariva AJ (1988) Electrochim Acta **33**: 1753
[9] Tilak BV, Perkins RS, Kozlowska HA, Conway BE (1972) Electrochim Acta **17**: 1447
[10] Sonehart P (1988) Electrochim Acta **13**: 1789
[11] Hepel M, Tomkiewiez M (1984) J Electrochem Soc **131**: 1288
[12] Valett G (1981) J Electroanal Chem **122**: 285
[13] Valett G (1982) J Electroanal Chem **138**: 37
[14] Valett G (1983) J Electroanal Chem **147**: 439
[15] Metikos-Hukovic M (1992) J Appl Electrochem **22**: 448
[16] Hills GJ, Sciffrin DJ, Thompson J (1974) Electrochim Acta **22**: 448

Received December 1, 1998. Accepted (revised) March 5, 1999